

## INJECTION BACKGROUND STUDIES AT FCC-ee

G. Nigrelli<sup>1,2,3\*</sup>, M. Boscolo<sup>2</sup>, G. Broggi<sup>3</sup>, R. Bruce<sup>3</sup>, Y. Dutheil<sup>3</sup>, B. Francois<sup>3</sup>, A. Frasca<sup>3,4</sup>,  
T. Mori<sup>5</sup>, A. Lechner<sup>3</sup>, G. Lerner<sup>3</sup>, F. Palla<sup>6</sup>, S. Redaelli<sup>3</sup>, K. Skoufaris<sup>3</sup>, S. Yue<sup>3</sup>

<sup>1</sup>Sapienza Università di Roma, Rome, Italy, <sup>2</sup>INFN-LNF, Frascati, Italy,

<sup>3</sup>CERN, Geneva, Switzerland, <sup>4</sup>University of Liverpool, Liverpool, UK,

<sup>5</sup>KEK, Tsukuba, Japan, <sup>6</sup>INFN Pisa, Pisa, Italy

### Abstract

The electron–positron Future Circular Collider (FCC-ee) is a proposed high-energy lepton collider designed to achieve unprecedented luminosity and precision in the study of fundamental particle physics. To fully exploit this potential, it is crucial to control beam-induced experimental backgrounds to ensure safe operation and optimal detector performance. This is particularly challenging due to the complex operational requirements; for example the top-up injection process that generates unavoidable losses at each injection while detectors are taking data. The present baseline scheme foresees a fast bump in the injection region that affects the full circulating beam, leading to additional beam-halo losses. In this paper, we study these losses, from their sources up to the detector using a multi-step simulation framework, employing multi-turn tracking followed by Monte-Carlo shower studies and detector occupancy analyses. The IDEA detector concept was used to evaluate their impact on vertex detector occupancy and compare them to the main luminosity background.

### INTRODUCTION

FCC-ee is a proposed 90.7 km electron–positron collider that will operate at four center-of-mass energies: the Z pole (45.6 GeV), the WW threshold (80 GeV), the ZH production peak (120 GeV), and the  $t\bar{t}$  threshold (182.5 GeV) [1]. Its design targets unprecedented luminosity through high beam currents and continuous top-up injection, required due to beam lifetimes well below one hour. This is possible thanks to a booster, compatible with all energies, so that energy ramps are not required in the collider. Injection is performed while the detectors are taking data, introducing a potential source of background. The Z pole is the most critical operating point for injection-induced backgrounds, featuring the highest beam currents ( $\sim 1300$  mA) and largest total stored beam energy ( $\sim 18$  MJ). Even a small fractional beam loss near the Interaction Regions (IRs) can deposit significant energy in the detectors. Experience at SuperKEKB has confirmed that backgrounds from injection losses can become a direct operational limitation [2, 3]. The injection scheme proposed for FCC-ee is even more challenging because it relies on a fast orbit bump that perturbs the circulating beam and enhances losses. The losses are mitigated by a global two-stage momentum and betatron collimation system in Point F (PF) [4], complemented by local tertiary collimators (TCT) upstream of the IRs.

\* giulia.nigrelli@cern.ch

This paper evaluates injection-induced losses at the Z pole using a multi-step simulation framework to quantify their impact on the detector occupancies.

### TOP-UP INJECTION SCHEME

At the Z pole, continuous top-up injection is performed every 3 s per beam, replenishing up to 10% of the stored (1200) bunches with 10% of the nominal bunch intensity ( $2 \times 10^{10}$ ), corresponding to approximately 1% of the total stored beam energy per injection. The baseline scheme relies on full off-energy, on-axis injection [5]: the injected beam is placed onto the chromatic orbit and synchronously damps until it merges with the stored beam. With a longitudinal damping time of 1179 turns, more than 8 damping times are available between consecutive injections.

The transverse separation between the injected and circulating beams at the injection septum is determined by the local optics,

$$|D_x \cdot \delta| = 5\sigma_{\text{circ}} + S + 5\sigma_{\text{inj}}, \quad (1)$$

where  $D_x$  is the periodic ring horizontal dispersion,  $\delta$  is the momentum offset of the injected beam,  $\sigma_{\text{circ}} = \sqrt{\beta\epsilon + (D\delta)^2}$  and  $\sigma_{\text{inj}} = \sqrt{\beta\epsilon}$  are the beam sizes of the circulating and injected beams respectively,  $\delta$  is the relative energy spread of the circulating beam, and  $S$  is the septum thickness. For the injected beam, the dispersion contribution to the beam size is neglected to simplify the solution of Eq. 1 and to reduce the required separation. However, this introduces a dispersion mismatch between the two beams, which drives betatron oscillation of the injected beam around the chromatic orbit.

For lattice version GHC\_V25.1 [6],  $D_x = -1.5$  m and  $\beta_x = 1000$  m, yielding an energy offset of  $\delta_{\text{offset}} = 0.95\%$ , close to the momentum acceptance of  $\sim 1\%$ . To satisfy Eq. 1, the stored beam is displaced toward the septum by a one-turn  $\pi$ -orbit bump generated by two kicker magnets, such that the entire circulating beam passes at  $5\sigma_{\text{circ}}$  from the septum. An absorber, yet to be designed, upstream of the septum intercepts particles that would otherwise be scraped there, concentrating losses away from the septum itself.

### SIMULATION FRAMEWORK

A three-step simulation workflow for beam-induced background (BIB) has been established, covering the full chain from tracking to detector occupancy estimates. In the first step, multi-turn beam tracking is performed using

Xsuite [7,8], with particle-matter interactions within collimators handled by the BDSIM library [9]. Surviving particles and newly produced stable charged particles are returned to Xsuite, and all collimator impacts are recorded. Aperture losses in the IRs are due to collimator out-scattering and not loaded in FLUKA to avoid double counting. In the second step, collimator hits in the proximity of the IR are used as input for dedicated electromagnetic shower simulations in FLUKA [10–12]. The FLUKA geometry is a detailed model of the FCC-ee IR, including both beamlines extending up to 700 m from the IP, and a schematic IDEA detector geometry [13]. Showers are propagated to the machine-detector interface (MDI). The MDI is defined as a cylindrical surface of radius 8 m and length 16 m centered at the IP enclosing the outer detector volume, and, within the detector, it follows the surface of the final focus cryostat and the beam pipe. Particle coordinates and momenta at the surface are stored. In the third step, MDI hits are passed to a full detector simulation based on Key4hep [14, 15], which is a comprehensive data processing framework supporting event generation, detector simulation and analysis. The IDEA detector concept [16] was considered for this study. It features a silicon pixel vertex detector and drift chamber tracker surrounded by a crystal dual-readout electromagnetic calorimeter within a superconducting solenoid, followed by a dual-readout fiber calorimeter, completed by a muon system in the iron yoke. In this study, the focus is on the vertex detector, which consists of three inner vertex barrel layers, middle and outer vertex barrel layers covering radius between 13.7 and 315 mm, and three disks per side.

The simulations with this complete framework are performed separately for the injected beam and the circulating beam. In addition, the step 1 results can be used to estimate the injection efficiency. For the injected beam, the initial distribution is matched to the chromatic closed orbit at the injection point using nominal booster parameters [5], without the dispersion contribution to the beam size. As only the positron line is available, only positrons have been simulated. Tracking is performed for 2500 turns with  $5 \times 10^5 e^+$  to evaluate injection efficiency, and for 700 turns with  $10^6 e^+$  to generate loss maps. For the circulating beam only the halo is considered, as the core is expected to be unaffected. A uniform distribution between  $5$  and  $11\sigma$  (the primary collimator aperture) is initialized in a dispersion-free region with  $5 \times 10^5 e^+$ , representing a conservative 1% of the total beam population. Particles are tracked for 100 turns following activation of the one-turn  $\pi$ -bump at turn 1.

## INJECTION-INDUCED BACKGROUND

The injection efficiency for lattice GHC\_V25.1 [6] is found to be 88%, as shown in Fig. 1, including beam-beam effects, synchrotron radiation, tapering, a detailed aperture model, and the full collimation system. When beam-beam effects are disabled, the efficiency exceeds 99%, identifying beam-beam interactions as the dominant loss mechanism: the beam-beam kicks drive injected particles beyond the

vertical dynamic aperture, resulting in losses that bypass the primary collimation insertion and deposit power at the vertical tertiary collimators upstream of the IPs.

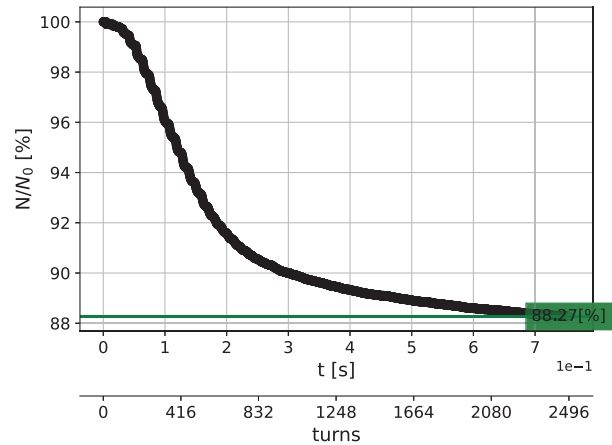


Figure 1: Injected beam population survival rate versus turn, showing an 88% injection efficiency after 2500 turns.

The simulated loss maps are shown in Fig. 2. For the injected beam (top), losses are concentrated in the main collimation insertion and at the IR collimators, with comparable or higher lost power at the latter. For the circulating beam halo (bottom), the one-turn  $\pi$ -bump scrapes approximately 50% of the modeled halo population: 30% is lost at the injection absorber while the bump is active, and the remaining 20% is distributed along the ring over subsequent turns, with losses at the IRs remaining lower than at the collimation insertion by approximately a factor of ten. For both simulations, TCT losses from the first step (tracking) are used as input to the second step of FLUKA shower simulations. Since all four IRs share the same layout and the TCT's impact distributions are comparable across turns and IPs, a generic IR is considered and all TCT's hits are superimposed. The particle flux at the MDI is dominated by photons in the external surface, with energies ranging from 10 keV to 10 GeV, centered around 1 MeV.

Each macro-particle tracked in Xsuite represents  $N_{inj}/N_{macro}$  real particles, where  $N_{inj} = N_{bunch}/10$  is the number of particles in the injected bunch and  $N_{macro}$  is the number of simulated macro-particles. The rate of particles hitting the MDI is then:

$$R_{MDI} = \frac{N_{inj}}{N_{macro}} \times n_{hit,TCT} \times \frac{\eta_{MDI}}{t_{rev}}, \quad (2)$$

where  $t_{rev} \approx 300 \mu s$  is the machine revolution period,  $n_{hit,TCT}$  is the TCT hit count per IP and  $\eta_{MDI}$  is the shower yield. We use either the turn-averaged value  $\langle n_{hit,TCT} \rangle_{turn} = N_{hit,TCT}^{tot}/(4 \cdot N_{turns})$ , or the maximum over all turns and IPs,  $n_{hit,TCT}^{max}$  to obtain  $\langle R_{MDI} \rangle$  and  $R_{MDI}^{max}$  respectively. The same procedure applies for the circulating beam halo, using  $N_{halo} = N_{bunch}/100$ . Applying Eq. 2:

$$\begin{aligned} \langle R_{MDI}^{inj} \rangle &= 0.35 \text{ GHz}, & R_{MDI}^{inj,max} &= 2.97 \text{ GHz}, \\ \langle R_{MDI}^{halo} \rangle &= 0.13 \text{ GHz}, & R_{MDI}^{halo,max} &= 0.48 \text{ GHz}. \end{aligned} \quad (3)$$

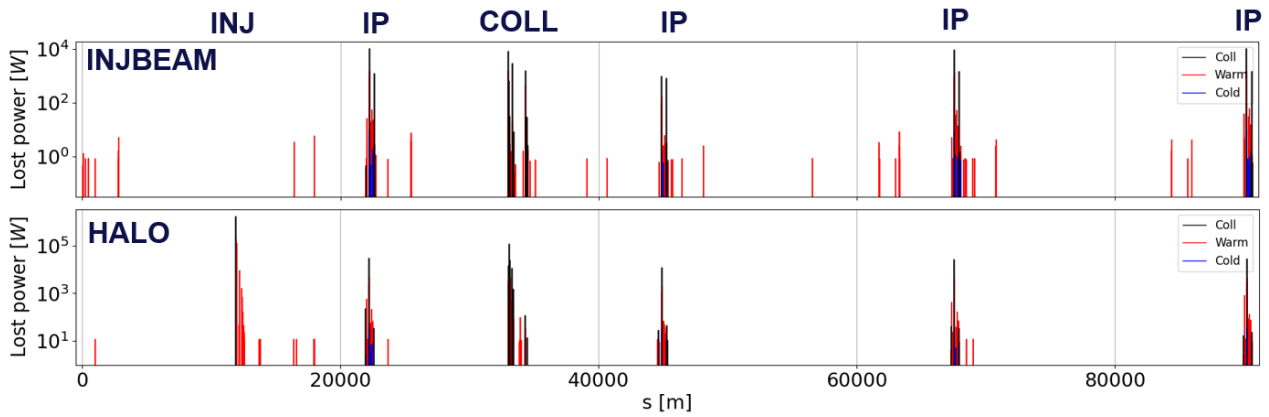


Figure 2: Longitudinal loss maps for the injected beam (top) and circulating beam halo (bottom), showing loss locations around the ring normalized to total power lost over the simulation duration (700 turns  $\sim$  0.2 s).

As a third step, the MDI hits are passed to the full IDEA detector simulation with two normalization weights. Since the TCT hit statistics are already encoded in the FLUKA sample, the average hit rate in each layer is calculated as:

$$R_{\text{layer}} = \frac{\langle n_{\text{hit}}^{\text{layer}} \rangle \cdot S}{A_{\text{sensor}} \cdot N_{\text{cells}}} \cdot \frac{R_{\text{MDI}}}{\eta_{\text{MDI}} \cdot N_{\text{hit,TCT}}}, \quad (4)$$

where  $\langle n_{\text{hit}}^{\text{layer}} \rangle$  is the average number of simulated hits per layer per event,  $A_{\text{sensor}} \cdot N_{\text{cells}}$  is the total sensitive area of the layer,  $S$  accounts for cluster size and a safety factor, and  $N_{\text{hit,TCT}}$  is taken as the mean (maximum) number of hits over all turns and IPs for the average (conservative) estimate.

Results are presented for the vertex barrel in Fig. 3, as it is the sub-detector most sensitive to direct particle hits. The Incoherent Pair Creation (IPC) background is shown for comparison as the dominant collision-induced background source, producing hit rates up to 200 MHz/cm<sup>2</sup> in the innermost vertex layer at the Z pole [16]. The occupancy is calculated assuming a conservative cluster size of 5 pixels per hit and a safety factor of 3, following the assumptions used in previous studies for IPC background. The innermost layer is consistently the most impacted across all contributions, as expected from the proximity to the IP. Both the average and maximum hit rates remain well below the IPC level across all layers. The maximum rate reached is approximately 8 MHz/cm<sup>2</sup> and 2 MHz/cm<sup>2</sup> in the innermost layer for injection-losses and halo-induced respectively, which is about one and two orders of magnitude below the IPC level. The turn-averaged rates are a further two orders of magnitude lower. As injection-induced backgrounds are well within the shadow of the IPC, they do not impose additional constraints on the vertex detector design.

## CONCLUSIONS

Injection-induced backgrounds at the FCC-ee Z pole have been evaluated for lattice GHC\_V25.1 using a three-step simulation framework combining multi-turn tracking, shower simulations, and full detector simulation. The simulated injection efficiency is 88 % when beam-beam effects are

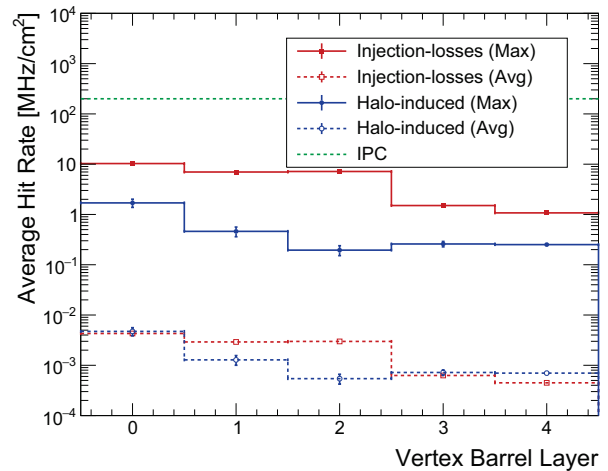


Figure 3: Average hit rate per layer in the IDEA vertex barrel for the injected beam (red) and circulating beam halo (blue), shown for both the average (dashed) and maximum (solid) MDI rates. The IPC level (green) is shown for reference.

included, identified as the dominant loss mechanism driving particles beyond the vertical dynamic aperture. In addition, during the one-turn  $\pi$ -bump, approximately 50 % of the modeled circulating beam halo is scraped, with 30 % lost at the injection absorber and the remainder distributed along the ring in the following turns. The resulting hit rates in the vertex barrel remain well below the IPC level of 200 MHz/cm<sup>2</sup> for both beam populations and both normalization weights. Injection-induced backgrounds are therefore not expected to pose a significant occupancy concern for the vertex detector under the current collimation and injection settings. Future work will focus on more realistic halo distributions, and a broader assessment of sub-detector impacts.

## REFERENCES

- [1] A. Abada *et al.*, “FCC-ee: The Lepton Collider, Future Circular Collider Conceptual Design Report Vol. 2”, *Eur. Phys. J. ST*, vol. 228, 2019.  
[doi:10.1140/epjst/e2019-900045-4](https://doi.org/10.1140/epjst/e2019-900045-4)

- [2] N. Iida *et al.*, “Beam Injection Issues at SuperKEKB”, in *Proc. IPAC'23*, Venice, Italy, 2023. doi:[10.18429/JACoW-IPAC2023-MOPL120](https://doi.org/10.18429/JACoW-IPAC2023-MOPL120)
- [3] H. N. Nakayama, T. Koga, K. Kojima, A. Natochii, and S. Vahsen, “Beam Background Measurements at SuperKEKB/Belle-II in 2020”, in *Proc. IPAC'21*, Campinas, Brazil, 2021. doi:[10.18429/JACoW-IPAC2021-WEXA07](https://doi.org/10.18429/JACoW-IPAC2021-WEXA07)
- [4] G. Broggi, “FCC-ee Collimation System Design”, Ph.D. thesis, Sapienza Università di Roma, 2026.
- [5] M. Benedikt, F. Zimmermann, B. Auchmann, *et al.*, “Future Circular Collider Feasibility Study Report”, *Eur. Phys. J. ST*, vol. 234, 2025. doi:[10.1140/epjs/s11734-025-01967-4](https://doi.org/10.1140/epjs/s11734-025-01967-4)
- [6] K. Oide, “Lattice progress and main parameters update”, presented at 202<sup>nd</sup> FCC-ee Accelerator Design Meeting, Geneva, Switzerland, 2025.
- [7] G. Iadarola *et al.*, “Xsuite: An Integrated Beam Physics Simulation Framework”, in *Proc. HB'23*, Geneva, Switzerland, 2023. doi:[10.18429/JACoW-HB2023-TUA2I1](https://doi.org/10.18429/JACoW-HB2023-TUA2I1)
- [8] A. Abramov *et al.*, “Collimation Simulations for the FCC-ee”, *JINST*, vol. 19, 2024. doi:[10.1088/1748-0221/19/02/T02004](https://doi.org/10.1088/1748-0221/19/02/T02004)
- [9] L. J. Nevay *et al.*, “BDSIM: An Accelerator Tracking Code with Particle–Matter Interactions”, *Comput. Phys. Commun.*, vol. 252, 2020. doi:[10.1016/j.cpc.2020.107200](https://doi.org/10.1016/j.cpc.2020.107200)
- [10] C. Ahdida *et al.*, “New Capabilities of the FLUKA Multi-Purpose Code”, *Front. Phys.*, vol. 9, 2022. doi:[10.3389/fphy.2021.788253](https://doi.org/10.3389/fphy.2021.788253)
- [11] G. Battistoni *et al.*, “Overview of the FLUKA Code”, *Ann. Nucl. Energy*, vol. 82, 2015. doi:[10.1016/j.anucene.2014.11.007](https://doi.org/10.1016/j.anucene.2014.11.007)
- [12] CERN, FLUKA WEBSITE. <https://fluka.cern>
- [13] A. Frasca *et al.*, “Radiation Environment at FCC-ee Experimental Insertion Regions”, *Phys. Rev. Accel. Beams*, to be published. doi:[10.1103/9j2q-zqxd](https://doi.org/10.1103/9j2q-zqxd)
- [14] G. Ganis, C. Helsen, and V. Völkl, “Key4hep, a Framework for Future HEP Experiments and its Use in FCC”, 2021, doi:[10.48550/arXiv.2111.09874](https://doi.org/10.48550/arXiv.2111.09874),
- [15] F. Gaede, M. Frank, M. Petric, and A. Sailer, “DD4hep: A Community Driven Detector Description for HEP”, *EPJ Web Conf.*, vol. 245, 2020. doi:[10.1051/epjconf/202024502004](https://doi.org/10.1051/epjconf/202024502004)
- [16] The IDEA Study Group, “The IDEA Detector Concept for FCC-ee”, 2025, doi:[10.48550/arXiv.2502.21223](https://doi.org/10.48550/arXiv.2502.21223),